

Probabilistic Evaluation of the Dynamics and Prediction of Supertyphoon Megi (2010)

CHUANHAI QIAN

*Nanjing University of Information Science and Technology, Nanjing, and National Meteorological Center, Beijing, China,
and Department of Meteorology, The Pennsylvania State University, University Park, Pennsylvania*

FUQING ZHANG AND BENJAMIN W. GREEN

Department of Meteorology, The Pennsylvania State University, University Park, Pennsylvania

JIN ZHANG

National Meteorological Center, Beijing, China

XIAQIONG ZHOU

NOAA/NCEP, College Park, Maryland

(Manuscript received 21 November 2012, in final form 21 July 2013)

ABSTRACT

Supertyphoon Megi was the most intense tropical cyclone (TC) of 2010. Megi tracked westward through the western North Pacific and crossed the Philippines on 18 October. Two days later, Megi made a sharp turn to the north, an unusual track change that was not forecast by any of the leading operational centers. This failed forecast was a consequence of exceptionally large uncertainty in the numerical guidance—including the operational ensemble of the European Centre for Medium-Range Weather Forecasts (ECMWF)—at various lead times before the northward turn. This study uses The Observing System Research and Predictability Experiment (THORPEX) Interactive Grand Global Ensemble dataset to examine the uncertainties in the track forecast of the ECMWF operational ensemble. The results show that Megi's sharp turn is sensitive to its own movement in the early period, the size and structure of the storm, the strength and extent of the western Pacific subtropical high, and an approaching eastward-moving midlatitude trough. In particular, a larger TC (in addition to having a stronger beta effect) may lead to a stronger erosion of the southwestern extent of the subtropical high, which will subsequently lead to an earlier and sharper northward turn.

1. Introduction

Over the past two decades, significant progress has been made in short-range forecasts of tropical cyclone (TC) tracks. Over the Atlantic basin, average track forecast errors for days 1–3 have been reduced by about 50% over the past 15 yr; average track forecast errors for days 4 and 5 have been reduced by 40% over the past 10 yr (Cangialosi and Franklin 2011). Similarly impressive improvements in TC forecasts have been observed over other regions, such as the western North Pacific

and southwestern Indian Ocean (Chan 2010). This progress is a result of advances in numerical weather prediction (NWP) and the multimodel consensus technique. Goerss (2000) showed that a simple average (or consensus) TC forecast derived from a combination of different models might be more accurate than the forecasts of the individual models. Currently, the National Hurricane Center uses several models as guidance in the preparation of official track and intensity forecasts (Cangialosi and Franklin 2011). These numerical models include global and regional dynamical models, statistical–dynamical models, consensus models, and even “weighted” or “corrected” consensus.

With the recent progress in computational power and data assimilation algorithms, ensemble forecasts have also been applied to TCs for both vortex initialization

Corresponding author address: Prof. Fuqing Zhang, Dept. of Meteorology, The Pennsylvania State University, 503 Walker Building, University Park, PA 16802-5013.
E-mail: fzhang@psu.edu

and probabilistic prediction (e.g., Buizza et al. 2007; Hamill et al. 2011; Zhang et al. 2009, 2010, 2011; Weng and Zhang 2012; Aksoy et al. 2012). For example, Zhang et al. (2011) used an ensemble-based data assimilation system to assimilate all available high-resolution airborne radar observations of North Atlantic TCs between 2008 and 2010 into convection-permitting numerical simulations; their results demonstrated improvements in both track and intensity forecasts. In September 2006, the European Centre for Medium-Range Weather Forecasts (ECMWF) implemented an operational 51-member ensemble system [1 control forecast and 50 perturbations; Buizza et al. (2007)] that provides routine forecasts of center position, minimum sea level pressure, and maximum surface wind for TCs around the globe. The National Centers for Environmental Prediction (NCEP), China Meteorological Administration (CMA), Japan Meteorological Agency (JMA), and other major national meteorological and hydrometeorological services (NMHSs) have also developed their respective TC ensemble prediction systems. These ensemble products have become increasingly important guidance for operational TC forecasting worldwide.

Despite the significant improvements in TC track prediction in recent years, large errors may still occur, especially so for some unusual cases. In particular, sharp track changes due to strong interactions between a TC and its environment could yield a highly inaccurate 3–5-day forecast that would result in unnecessary warnings and an improper allocation of emergency management resources—a major problem in the case of an intense supertyphoon such as Megi (or, as demonstrated by Hurricane Sandy in 2012, when a TC strikes a highly populated area). The main goal of this study is to investigate how the interaction between Supertyphoon Megi (2010) and its immediate environment impacted its subsequent track over the western North Pacific. The primary data used for this study are derived from The Observing System Research and Predictability Experiment (THORPEX) Interactive Grand Global Ensemble (TIGGE; Bougeault et al. 2010) dataset, which are provided by many international centers and are stored in (WMO) gridded binary (GRIB-2) format in archive centers at CMA, ECMWF, and the National Center for Atmospheric Research (NCAR). Only ECMWF single-level and pressure-level¹ data are selected and downloaded from the TIGGE dataset. The

ECMWF ensemble data are available in a thinned Gaussian grid (N200, equivalent to a horizontal spacing of ~30 km in the vicinity of Megi). The initial perturbations of the ECMWF ensemble were generated using the singular-vector technique to represent the uncertainties in the operational analysis (Buizza et al. 2007).

An overview of Megi and its forecasts is presented in section 2. Major findings on the uncertainty and dynamics of track prediction as revealed by the ECMWF ensemble are shown in section 3. A summary and discussion are given in section 4.

2. Overview of Supertyphoon Megi (2010)

At 0000 UTC 13 October 2010, a tropical depression formed over the western North Pacific far to the east of the Philippines (Fig. 1a); 12 h later, the depression had strengthened sufficiently to be named Tropical Storm Megi. The TC strengthened as it moved northwestward over the next 3 days and became a severe typhoon [maximum sustained surface winds near TC center of at least 41.5 m s^{-1} ; Qian et al. (2006)] at 1200 UTC 16 October. Megi then moved west-southwestward and continued to strengthen, reaching its peak intensity by 1200 UTC 17 October (Fig. 1b), with a minimum central pressure of 895 hPa and maximum winds up to 72 m s^{-1} ; this intensity made Megi the strongest TC in any basin during 2010, and also the strongest western North Pacific TC in over 20 yr. Megi made landfall in the northeastern Philippines as a supertyphoon (maximum sustained surface winds of at least 51.0 m s^{-1}) at 0425 UTC 18 October, causing 11 deaths, 16 injuries, and 200 000 evacuations. The TC gradually weakened as it crossed the northern Philippines and emerged in the South China Sea, at which point it was still moving west (albeit more slowly). At 0000 UTC 20 October, Megi suddenly turned almost 90° to the right and headed due north. Megi made landfall over southern Fujian Province in China as a typhoon at 0455 UTC 23 October, and then rapidly weakened to a tropical depression by 1800 UTC 23 October.

a. Left bias in official track forecasts

The observed best track of Megi can be divided into three stages (Fig. 1a): the northwestward movement from genesis through 16 October (stage 1), the west-southwestward movement from 17 through 19 October (stage 2), and the northward movement from 20 to 24 October (stage 3). The sudden track change on 20 October posed major challenges to operational forecasters. Figure 2 shows the official track forecasts from three operational typhoon centers: CMA, the Joint Typhoon Warning Center (JTWC), and JMA. These

¹For ECMWF ensemble forecast data from TIGGE, nine pressure levels were available: 1000, 925, 850, 700, 500, 300, 250, 200, and 50 hPa. Note that the only variable available at 50 hPa is geopotential height.

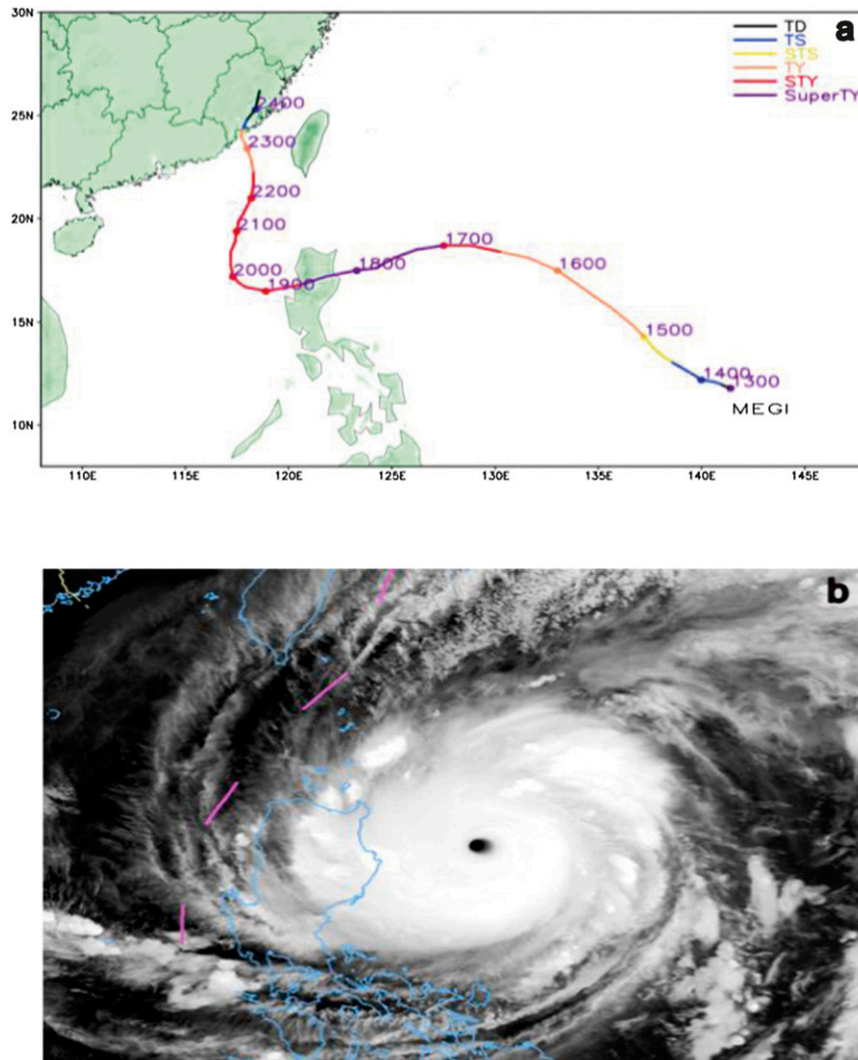


FIG. 1. Observations of Supertyphoon Megi. (a) Best track (as determined by CMA) between 13 and 24 Oct 2010. (b) Infrared satellite imagery from the *National Oceanic and Atmospheric Administration-18 (NOAA-18)* satellite at 1805 UTC 17 Oct, around the time of peak intensity.

operational centers issued 5-day track forecasts every 6 h (at 0000, 0600, 1200, and 1800 UTC) during Megi's life cycle. During stage 1, the official forecast tracks issued by the three centers are both consistent and very close to the observed track. As a whole, the track forecast errors from days 1 to 5 are relatively small in the first stage. However, nearly all of the CMA, JTWC, and JMA official 5-day track forecasts issued throughout most of stage 2 overpredicted the westward motion (Qian et al. 2012), resulting in large errors when Megi turned sharply to the north over the South China Sea. The official track forecasts continued to have somewhat leftward bias during stage 3, after the observed storm headed to the north.

b. Uncertainty in ECMWF ensemble forecasts

As one of the most sophisticated, reliable, and accurate operational NWP models, the ECMWF model is highly respected and utilized by operational forecasters. The ECMWF TC track ensemble forecasts are available in real time to CMA and have provided extremely helpful guidance for TC forecasting and warning operations at CMA.

As shown in Fig. 3, at the beginning of a 4-day period starting 1200 UTC 13 October, the ECMWF 5-day ensemble forecasts exhibit reasonable skill in forecasting Megi's track. Nearly all ensemble members are highly concentrated and the ensemble average is close to the

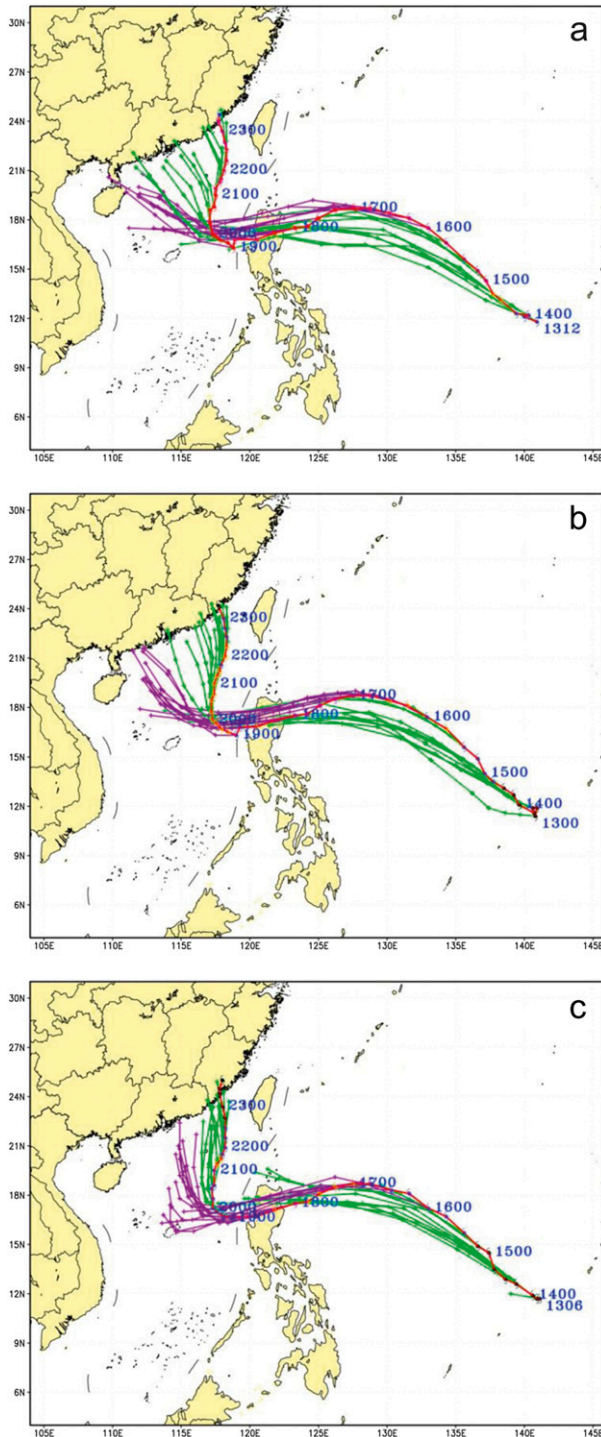


FIG. 2. Official track forecasts of Megi by (a) CMA, (b) JTWC, and (c) JMA at 6-h intervals. Green lines are track forecasts at different initial times, with stage 2 (17–19 October) highlighted by purple lines; the red line is the real-time observed positions estimated by each of the three typhoon centers (note that the three typhoon centers upgraded Megi to a tropical storm at different synoptic times on the same day).

deterministic forecast; all of these forecasts are close to the observed best-track estimate by CMA (<http://www.typhoon.gov.cn/index.php?controller=spage&pid=170>), indicating little uncertainty in the track forecast during this stage. It is important to note that at 1200 UTC 16 October, the forecasts from most members are still quite accurate through 48 h; beyond this time, track errors increase greatly as the majority of the ensemble members fail to predict the sharp northward turn.

The ensemble forecasts initialized at 1200 UTC 17 October (Fig. 3e) exhibit dramatic divergence, representing great uncertainty in the future track of Megi. While some members still continue to move westward or northwestward, others predicted the storm to turn to the north. Additionally, the deterministic forecast differs significantly from the ensemble mean. Although the spread of track forecasts remains large over the next 2 days (Figs. 3f and 3g), more and more ensemble members forecast the northward turn. After the turn occurred at 1200 UTC 20 October (Fig. 3h), the ensemble spread decreased and the deterministic forecast nearly overlays both the ensemble average and the observed best-track estimate.

The official forecasts by all three leading operational forecast centers mentioned in section 2a mostly failed to predict Megi's sharp northward turn beyond a lead time of 1 day. Although ECMWF ensemble members began to signal the turn as early as 1200 UTC 17 October, the uncertainty associated with the tremendous ensemble spread gave operational forecasters little confidence that this scenario would verify. Many important questions arose from the failure to accurately forecast the track of Megi. This study will attempt to answer some of these questions, by investigating the causes of the storm's sudden track change, the forecaster's judgment under inherent uncertainties of the numerical guidance, and the lessons learned from this unusual case for predicting future extreme events at the operational forecast centers.

We will be using the ensemble sensitivity methodology first used in Zhang (2005) and subsequently extended in Hawblitzel et al. (2007), Sippel and Zhang (2008, 2010), Melhauser and Zhang (2012), and Munsell et al. (2013) for studying various phenomena that include winter cyclones, summertime mesoscale convective vortices, and tropical cyclones. A similar ensemble sensitivity technique was developed in Ancell and Hakim (2007), which was recently adopted in Chang et al. (2013). The former approach (used in this study) relies directly on the ensemble correlations/covariances or direct comparison between good and poor members while the latter approach (Ancell and Hakim 2007) relies exclusively on the linear regression based on the ensemble correlations.

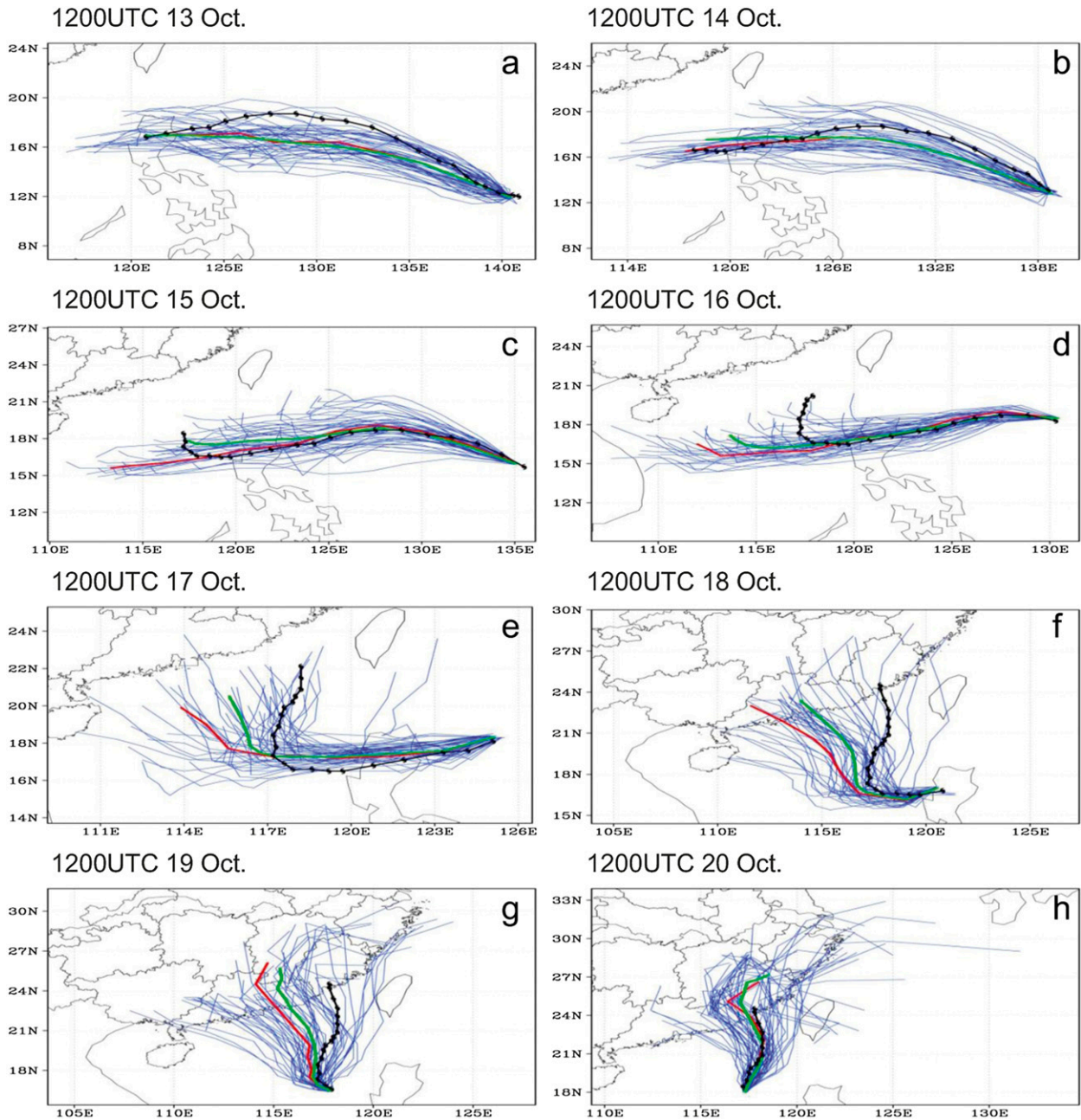


FIG. 3. ECMWF 5-day ensemble forecasts initialized at 1200 UTC from (a) 13 Oct through (h) 20 Oct 2010 (i.e., every 24 h). The red line is the deterministic (operational) forecast, blue lines are the forecasts from each of the 51 ensemble members, the green line is the ensemble mean, and the black line is the observed best track.

3. Results

a. Differences in TC tracks of ensemble members prior to the sudden northward turn

As shown in Fig. 3e, about half of the 51 members from the ensemble forecast initialized at 1200 UTC 17 October show a northward-moving component (including two outliers that turned north too early) while the other half

continued to go westward, as in the deterministic forecast. A sample of 20 members were divided subjectively into two groups (Fig. 4): the “good” group consists of the 10 members that had the smallest mean track forecast errors verified against the best track (all of which correctly predicted the northward turn), and the “poor” group, which consists of the 10 members that had persistent westward motion and the largest mean track errors.

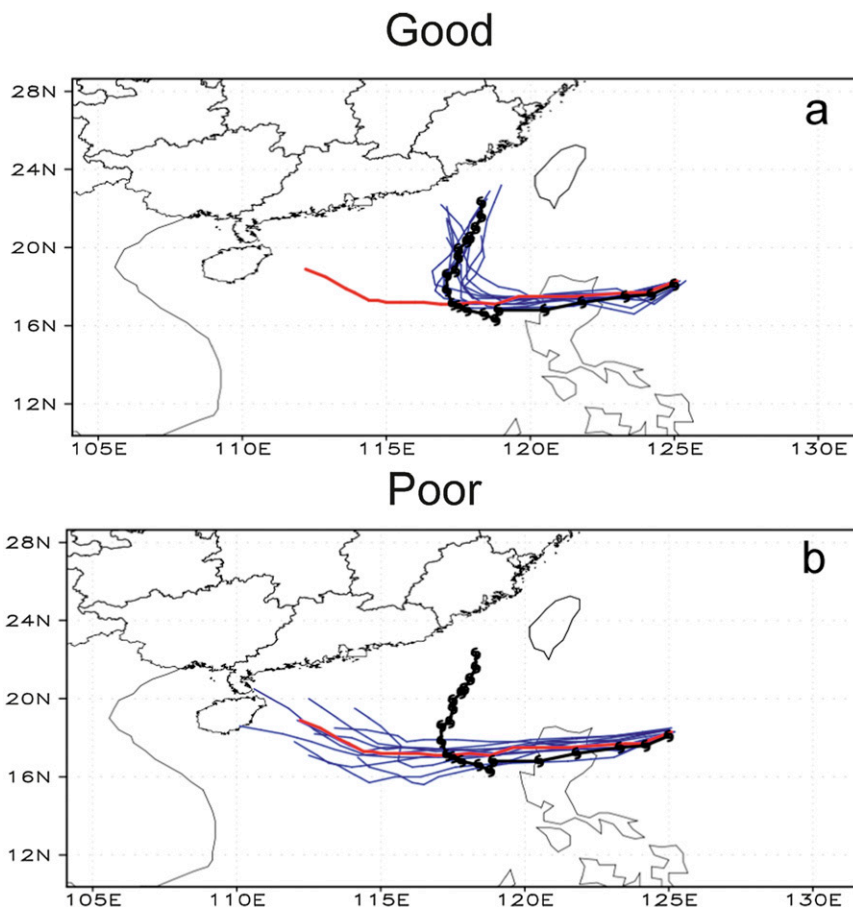


FIG. 4. The 5-day track forecasts from (a) 10 good members (1, 2, 6, 7, 11, 19, 23, 31, 41, and 46) and (b) 10 poor members (4, 5, 16, 17, 20, 28, 32, 36, 37, and 45) selected from the ECMWF ensemble forecast initialized at 1200 UTC 17 Oct 2010. The red line is the deterministic forecast (operational forecast), blue lines are the forecasts from the individual ensemble members, and the black line is the observed best track.

Composites (averages) of the 500-hPa height fields for these two groups are shown in Fig. 5. Initially, the mean TC centers of the groups overlap nearly perfectly. The centers of the poor members then moved westward more quickly than the centers of the good members. Over the first 48 h of the forecast, the distance between the centers of the two groups increased gradually to 1.2° in longitude; in the subsequent 12 h (as Megi approached the turning point), the separation rose to nearly 2.0° in longitude (the centers of both groups were at the same latitude throughout the first 60 h). Similar features were also evident on other pressure levels, such as 925, 850, and 700 hPa (not shown).

A scatterplot of TC movement during the first 24 h versus the sum of the track forecast errors at 72, 96, and 120 h^2 (using all 51 members; Fig. 6) was made to test the

relationship between Megi's early movement and its later track. Basically, track forecast errors are a proxy for verifying the sharp northward turn, with larger error representing a failure to forecast the turn. Looking at Fig. 6, TC movement during the first 24 h has a strong linear relationship with later track forecast error, with a correlation coefficient of 0.54 that is significant above the 99% confidence level. The mean moving speed of the typhoon is 15.7 km h^{-1} for the good group and 20.0 km h^{-1} for the poor group. This quantitatively confirms what is shown in Fig. 5: ensemble members with more slowly moving TCs in the first 24 h were able to correctly forecast the later northward turn. Similar linear relationships were also evident when the window was expanded from 24 h to 36, 48, or 60 h (not shown). Clearly, Megi's sharp change in track is related to the movement during the first 24-h forecast initialized from 1200 UTC 17 October, even though it is not clear what contributes to the slow movement of the typhoon in the early period.

² Summing the track errors over these three times acts to provide a smoother, longer-term measure of track error.

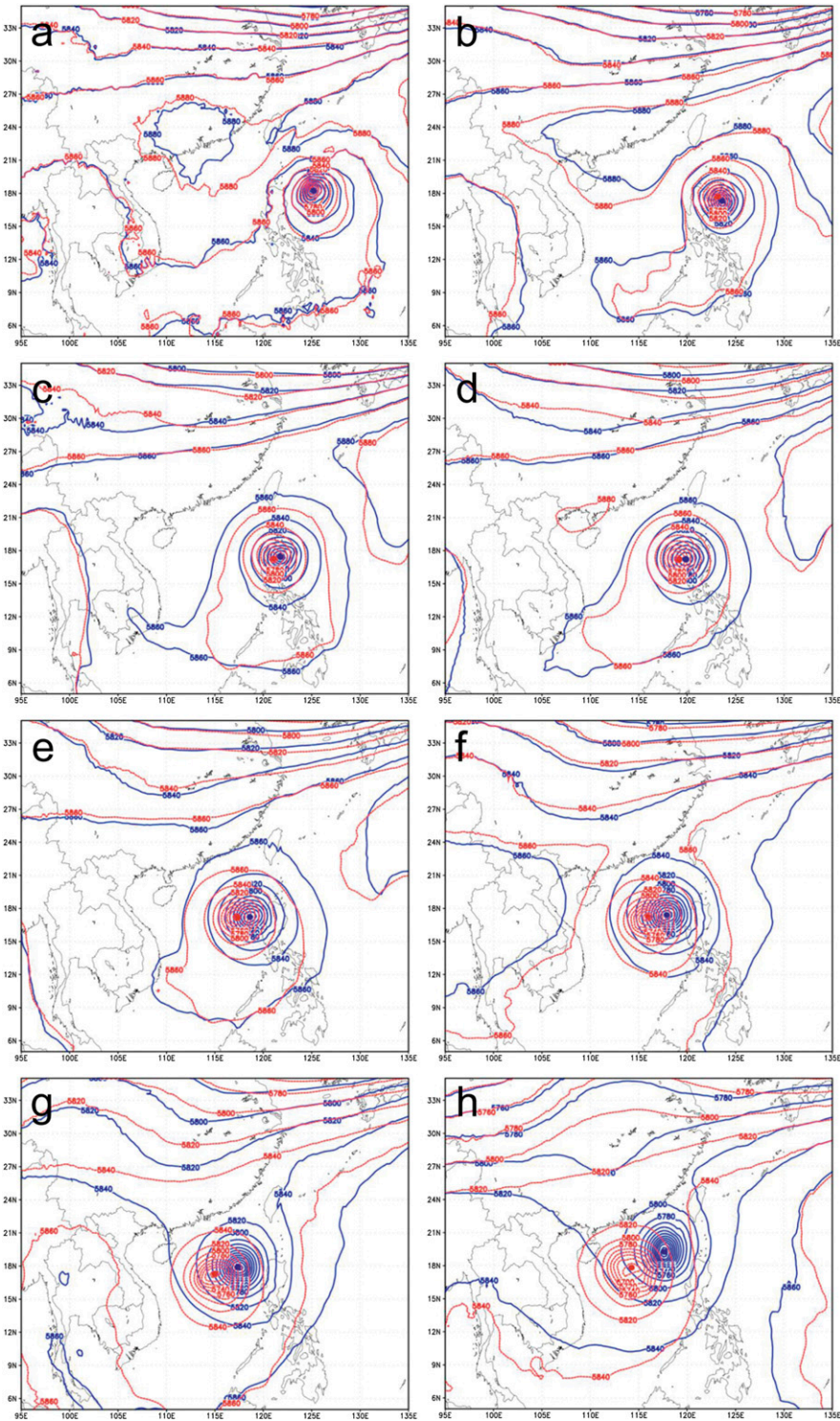


FIG. 5. Averaged 500-hPa heights of the 10 good members (blue) and 10 poor members (red) for lead times of (a) 0, (b) 12, (c) 24, (d) 36, (e) 48, (f) 60, (g) 72, and (h) 96 h.

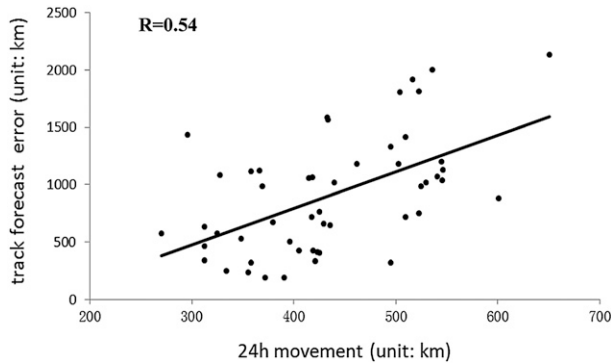


FIG. 6. Scatterplot of TC movement between 1200 UTC 17 and 1200 UTC 18 Oct 2010 vs the sum of the 72-, 96-, and 120-h track forecast errors (both axes in km) for each of the 51 ECMWF ensemble members initialized at 1200 UTC 17 Oct. 2010.

A correlation analysis between TC movement over the first 24 h and the 120-h 500-hPa height field was performed to further examine the potential influence of the TC's early westward movement on the subsequent motion. The results (Fig. 7) show an area of positive correlation over the northeastern South China Sea, Taiwan Island, and southeastern mainland China; an area of negative correlation is evident over the northwestern South China Sea, Hainan Island, and northern Vietnam. Although correlation does not necessarily imply causality, this distribution of correlations suggests that a slower westward motion of Megi in the 24 h after 1200 UTC 17 October might have contributed to the lower 500-hPa heights over the northeastern South China Sea and Taiwan at 120 h (1200 UTC 22 October). In line with the results from Figs. 5 and 6, a slower movement in the first 24 h is favorable for the sharp northward turn a few days later.

b. Differences in TC size of ensemble members prior to the sudden northward turn

Figure 5 suggests that there are significant differences in TC size between the good and poor groups. Analyses within the framework of a moving vortex are performed to further study the impact of TC size—defined as the distance from the center to the outermost closed contour of geopotential height at 700 hPa—on track change. The composite 700-hPa heights of the good and poor groups are shown in Fig. 8. At the initial time (1200 UTC 17 October), the storms in both groups were nearly the same size (Fig. 8a). A day later, the good members have larger TCs than the poor members, especially in the western semicircle (Fig. 8b). The size difference between the two groups continued to increase (particularly to the north and west) over the next 48 h, reaching a peak at 72 h (Fig. 8d). The closed 3120-m

isohypse at 700 hPa for the good group extends up to 2.5° to the north of that for the poor group. Such results suggest that the size of a TC could influence its own movement through the circulation-induced steering flow and interactions with the surrounding environment.

For example, a larger circulation of a TC vortex may induce additional advective contributions to the northward motion as a result of the so-called β -effect propagation—that is, a nonlinear advection of the symmetric TC vortex by the quasi-uniform flow in the central region of a weak azimuthal wavenumber 1 asymmetry induced by β , the meridional variation of the Coriolis parameter (e.g., Adem and Lezama 1960; Anthes and Hoke 1975; Chan and Williams 1987; Fiorino and Elsberry 1989). The magnitude and, to some extent, the direction of β -effect propagation depends substantially on the TC outer-wind structure: a larger outer circulation may yield a greater northward component of motion. Moreover, as shown in the recent study of Fang and Zhang (2012), the β effect may also vary with different heights and time that will further impact the TC movement and vertical wind shear at different stages of the TC evolution. Even without environmental mean flow, the β effect may first lead the TC vortex northwestward but eventually the storm will curve north and then northeast (Fang and Zhang 2012). However, it is beyond the scope of the current study to differentiate the relative contributions of the β effect to the northward movement of Megi from other mechanisms to be described in the following sections.

c. Interactions between the TC and the subtropical high

The strength of the subtropical high (SH) has a major impact on the TC motion (Elsberry 1987; Colbert and Soden 2012): a TC moves westward more quickly when there is a stronger SH to the north. As shown in Figs. 5 and 8, there are initially no major differences in SH strength between the good and poor groups. As time elapses, the poor group has a stronger SH than the good group;³ this could be deduced from the notion that the bigger TC size of the good group has a greater “erosion” effect on the SH. In other words, larger TCs have a broader area of lowered heights that overlap more with the SH, which would naturally weaken both the outer edges of the SH as well as the steering flow. Such an erosion mechanism could be one of the main reasons

³ The strength of SH in this study is defined in terms of the “westward expansion (to the north of the TC)” or the integrality of a band-shaped SH to the north of the TC rather than the maximum intensity of the SH.

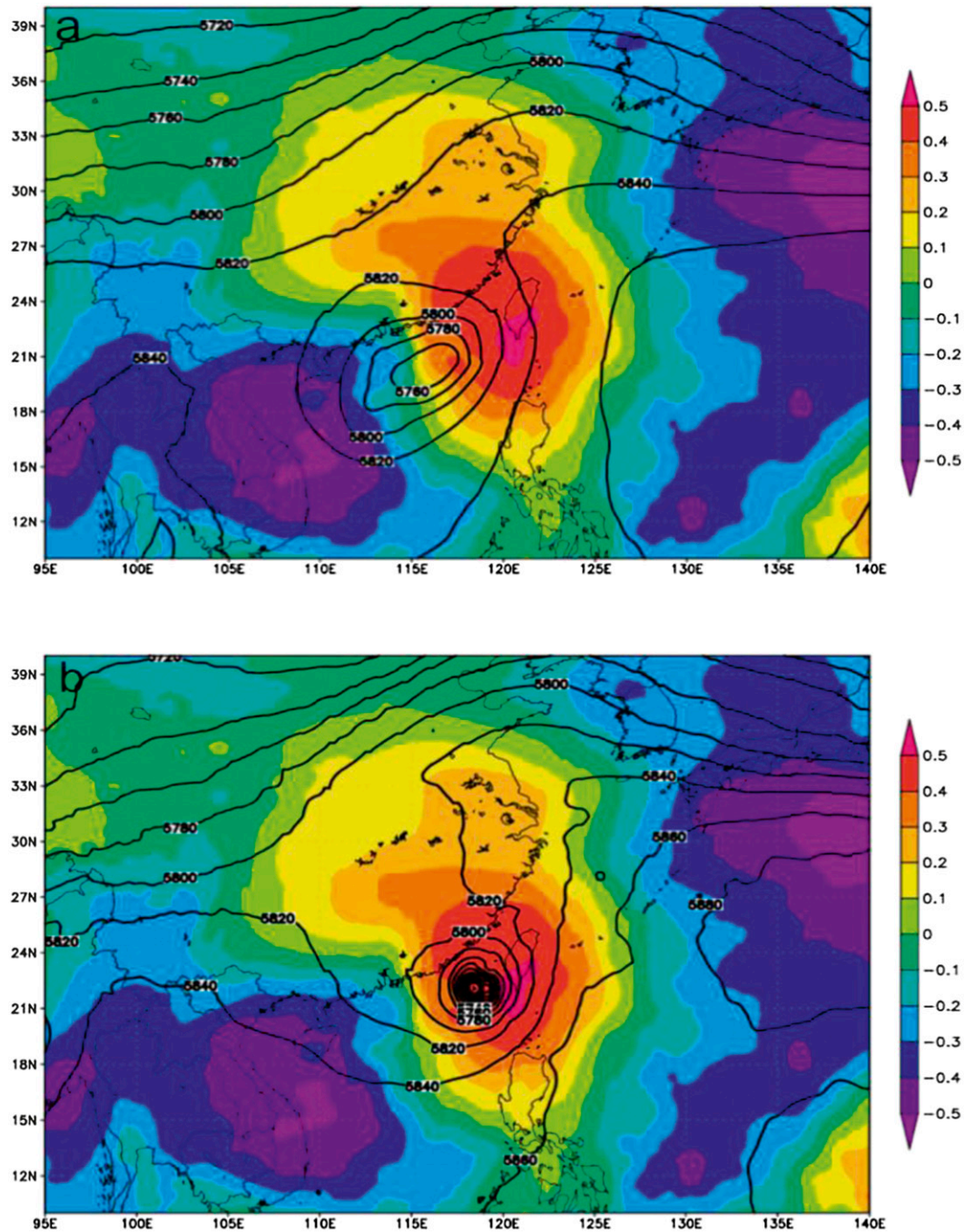


FIG. 7. Correlation (color fill) between TC movement during first 24- and 120-h 500-hPa heights (i.e., valid at 1200 UTC 22 Oct 2010). Black contours show 500-hPa heights for (a) the ensemble mean of the forecast initialized at 1200 UTC 17 Oct (valid at 1200 UTC 22 Oct) and (b) the analysis at 1200 UTC 22 Oct.

that the good members move more slowly than the poor members.

Looking at Fig. 8, the strength of the SH (as measured by the maximum 700-hPa height to the north of the TC) for both good and poor members decreases over time

from 3180 to 3140 m. There is a difference, however, between the two groups in the structure of the SH to the north and northeast of the TCs: by 72 h (Fig. 8d), a break (erosion) in the SH is evident in the good members but not in the poor members. The break in the

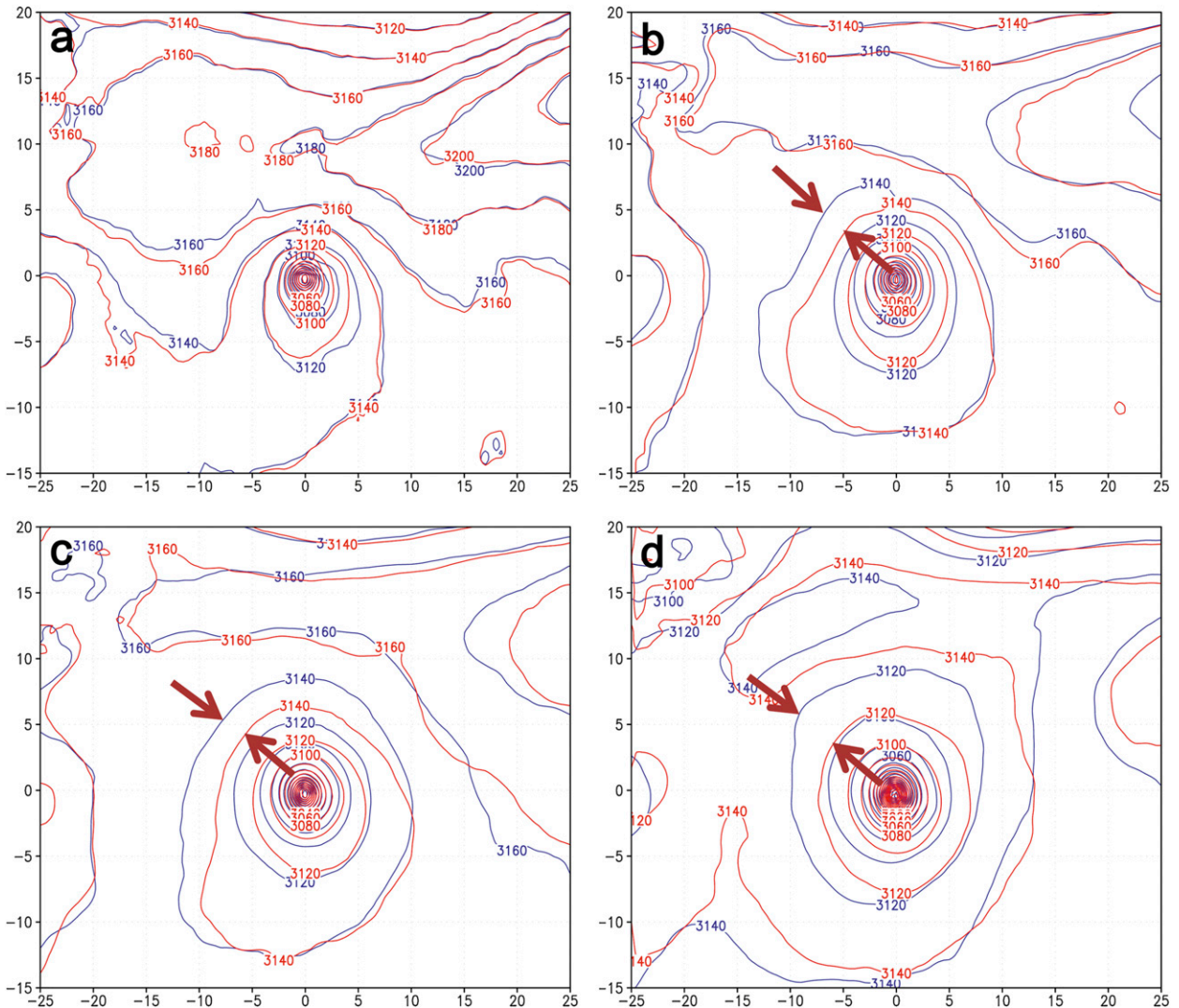


FIG. 8. Averaged 700-hPa heights of the 10 good members (blue) and 10 poor members (red) in vortex-centered coordinates for lead times of (a) 0, (b) 1, (c) 2, and (d) 3 days from forecasts initialized at 1200 UTC 17 Oct 2010. Arrows show the difference in TC size between the two groups.

SH allowed the TCs in the good members to turn to the north, whereas the stronger uneroded SH in the poor members continued to (erroneously) steer the TCs westward.

Brennan and Majumdar (2011) showed significant differences in the ultimate track of Hurricane Ike in ensemble members that initially displayed only small differences in the strength of the Atlantic SH. As mentioned in section 3a, the slower movement of the good members has already started within the first 24 h of the forecast, yet during this period there is no discernible difference in the SH between the good and poor members. Nevertheless, even subtle differences in the SH in the initial or early conditions may be the root difference

of the later forecast divergence. The similarity between Megi and Ike underscores the strong sensitivity of the subsequent track forecast to small initial differences in the SH, despite the fact that the two TCs were in different basins.

In addition to focusing on the good and poor members, the impact of SH strength on TC motion could also be verified with the two outlier members that have the earliest northward movement (Fig. 3e). At the initial time and thereafter, the outlier members on average have weaker subtropical highs than the good members (not shown). A weaker and more eastward-located subtropical high allowed the TCs in these outlier members to turn earlier than the good members.

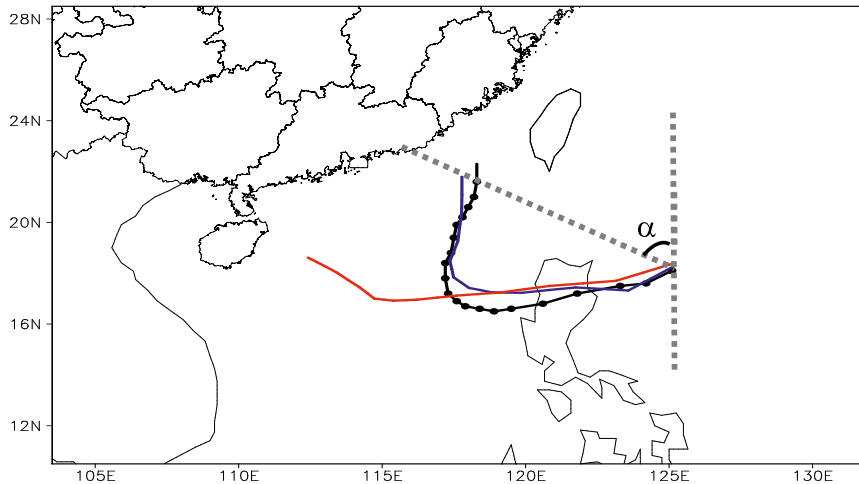


FIG. 9. Turning angle α . The solid line with dots denotes the best track of Megi between 1200 UTC 17 and 1200 UTC 22 Oct 2010. The 5-day forecast tracks averaged over the 10 good (poor) members are shown in blue (red).

d. Correlation between turning angle and 500-hPa height

Because the area of positive correlation between the early movement and the 120-h 500-hPa height is collocated with Megi's actual position at 1200 UTC 22 October (Fig. 7b), it is uncertain as to whether or not the storm's track change was related to its intensity. Nevertheless, the sharpness of the northward turn suggests that there may have been some dramatic changes in the environment or the structure of the TC itself. To examine the relationship between such changes and the sharp northward turn, a turning angle α (Fig. 9) is defined as

$$\alpha = \tan^{-1} \frac{\text{lon}_0 - \text{lon}_1}{\text{lat}_0 - \text{lat}_1}, \quad (1)$$

where lon and lat denote the longitude and latitude of the TC center at 1200 UTC 17 October (subscript 0) and 1200 UTC 22 October (subscript 1). For a given ensemble member, a smaller α corresponds to a more northward track. The correlations between α and 500-hPa heights (within the framework of a moving vortex) for ensemble forecasts initialized at 1200 UTC 17 October were calculated for lead times ranging from 12 to 72 h (Fig. 10). Over the first 24 h (Figs. 10a and 10b), the correlation is statistically significant over the TC region except at the TC center; thus, the track change is closely related to the TC's outer circulation but not to its intensity. The positive correlation (at these early times) between α and 500-hPa heights in the outer region of the TC indicates that larger storms tend to move more northward.

Meanwhile, a trough initially to the northwest of Megi (Fig. 10b) moves toward the TC and develops (Figs. 10c–f). The positive correlation area associated with the trough merges with the positive correlation areas associated with Megi between 36 and 72 h (Figs. 10c and 10f). The distribution of correlation and the evolution of the trough show that a deeper trough is more favorable for Megi to turn sharply to the north (i.e., have a smaller turning angle).

The plausible dynamic explanation of how Megi's structure could lead to its later track change lies in strong interaction between the TC and the SH. Between 12 and 24 h (Figs. 10a and 10b), the SH—as measured by the 5880-m isohypse—shifted eastward away from Megi, resulting in lower heights to the north of the TC. Consequently, the easterly steering flow weakened and slowed TC movement. At the same time, the SH also began to build southward, trapping Megi in a nearly stationary “saddle” pattern (Fig. 10e). The approaching trough, however, continued to lower heights to the north of the TC (Figs. 10e and 10f), creating an opening through which the storm could move northward. The southward-building SH east of Megi also contributes to the southerly steering flow at the time of the sharp turn (Fig. 10f), consistent with the negative correlation area over the SH.

e. Analysis of steering flows

Even though present-day TC operational forecasters can obtain substantial guidance from various NWP models, they still use steering-flow theory to judge the speed and direction of storm movement. In forecasting, a great deal of research focuses on the relationship

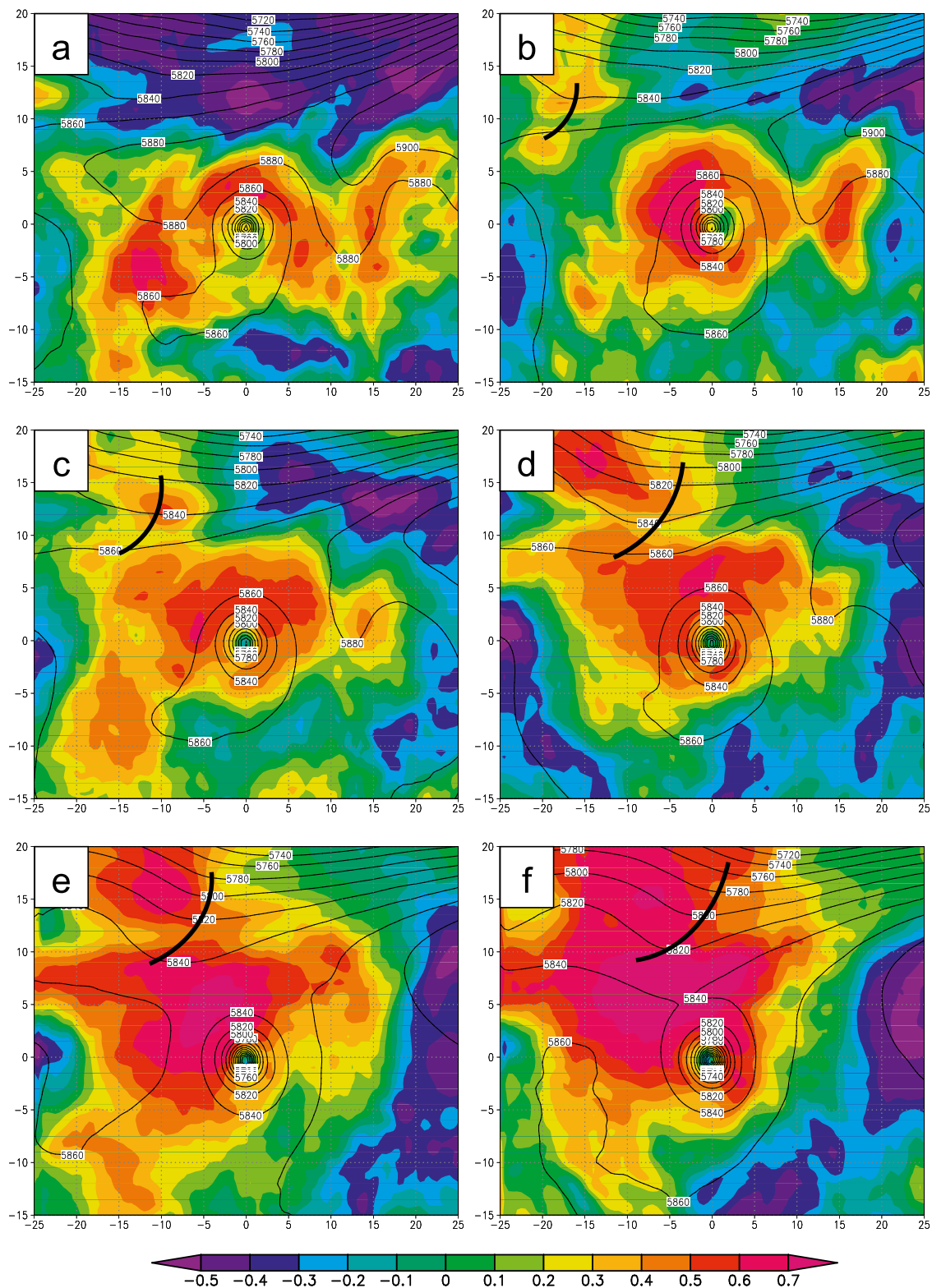


FIG. 10. Correlation (within a vortex-following framework) between α and 500-hPa heights for the 51-member ECMWF ensemble forecast initialized at 1200 UTC 17 Oct 2010, for lead times every 12 h between 12 and 72 h.

between the TC movement and the surrounding large-scale circulation. Chan and Gray (1982) found that the midtropospheric flow (500–700 hPa) in a 5° – 7° (of latitude) annulus from the TC center has the best correlation with cyclone movement. Dong and Neumann (1986) and Velden and Leslie (1991) investigated the basic relationship between TC intensity and the depth of the environmental steering layer for the Atlantic and Australian basins, respectively. They reached similar conclusions: lower-tropospheric layer averages are best correlated with future motion for weak and moderate TCs, whereas deep-layer steering generally is more appropriate than single-level steering for more intense storms. In other words, the depth of the steering layer increases with TC intensity.

At its peak, Megi reached supertyphoon intensity (the same as a category 5 hurricane on the Saffir–Simpson hurricane wind scale) and maintained severe typhoon status even after striking the northern Philippines and entering the South China Sea. Because Megi was so intense, we calculated the deep-layer mean (DLM) steering flow⁴ over a 5° – 7° annulus around the TC using ECMWF ensembles initialized at 1200 UTC 17 October. As shown in Fig. 11, the DLMs for both good and poor members match well with their tracks and moving speeds (see Fig. 4). During the first 24 h (Figs. 11a–c), both groups have westward-steering vectors with almost the same speed of $\sim 4 \text{ m s}^{-1}$. At 36 h (Fig. 11d), the DLM of the good group (DLM-G) is a bit slower than the DLM of the poor group (DLM-P); by 48 h (Fig. 11e), both DLMs have slowed to $\sim 2 \text{ m s}^{-1}$ but their *difference* increases to 0.6 m s^{-1} . This difference is consistent with Fig. 4, which shows that the good members move more slowly than the poor members prior to the time of the northward turn. At 60 h, however, DLM-G's vector changes significantly, turning to the north-northwest at an even smaller magnitude of 0.7 m s^{-1} . The DLM-G vector points to the north by 72 h (1200 UTC 20 October; Fig. 11g), at which time Megi was heading almost due north. The DLM-P vector, on the other hand, continues to point to the west through 72 h. By 96 h, both DLM-G and DLM-P have turned more to the right and increased in magnitude. Overall, the differences between the DLM-G and DLM-P vectors are consistent with the differences in TC motion between the good and poor members.

4. Summary and discussion

Global and regional numerical weather prediction models and ensemble techniques are making continuous

progress in providing increasingly trustworthy real-time operational guidance, including for TC track forecasts. Nevertheless, these models can become unreliable in some complicated synoptic situations; in such instances, forecasters face major challenges in using numerical guidance to make a reasonable and accurate forecast. An example of an unusually difficult track forecast is Supertyphoon Megi, which made a sharp northward turn that was not predicted in official forecasts. At 1200 UTC 17 October (3 days before the sharp turn), the track spread of the ECMWF 51-member ensemble forecast indicated significant uncertainty; some “good” members correctly signaled the northward turn and other “poor” members took Megi on a persistent westward track.

Megi's sudden northward turn was likely the result of interactions between the TC and its surrounding environment. Therefore, to elucidate the factors most crucial to the turn, the TC structure and environmental conditions of the aforementioned good and poor members are compared. It is found that the good members have larger TCs, a weaker subtropical high, and a slower westward motion. The relationship between these characteristics is straightforward: larger TCs are able to more strongly “erode” the subtropical high, resulting in a weaker steering flow and thus a deceleration in TC forward speed. An eastward-moving trough also contributed to Megi's sharp turn by further eroding the subtropical high. The amplitude and location of the trough is nearly identical between the good members and the poor members from the initial time to 36 h (Fig. 5); at later times, the poor members have a slightly weaker and slower trough. It is indeed possible that even if the trough was correctly forecasted, the more westward track of Megi in the poor members would have kept the TC too far south and west to feel the impact of the trough.

An analysis of the correlation between the storm's turning angle and 500-hPa height suggests that TC *intensity* is not as important as *size* in determining track. Calculations of steering flow were consistent with TC tracks in the various members; in particular, a northward component was evident in the good members but absent in the poor members.

Research has suggested that ensemble mean forecasts, or consensus forecasts derived from multiple numerical models, may be (on average) more accurate than the forecasts of individual models (Goerss 2000). In operational situations, however, forecasters sometimes have a habit of placing too much weight (and in a few cases full weight) on the deterministic forecast. The case of Megi illustrates the dangers of such a practice: for ECMWF forecasts initialized from 17 to 20 October (Figs. 3e–h), the ensemble means (though not perfect)

⁴The DLM steering flow was computed by taking a simple average of the winds at 925, 850, 700, 500, 300, 250, and 200 hPa.

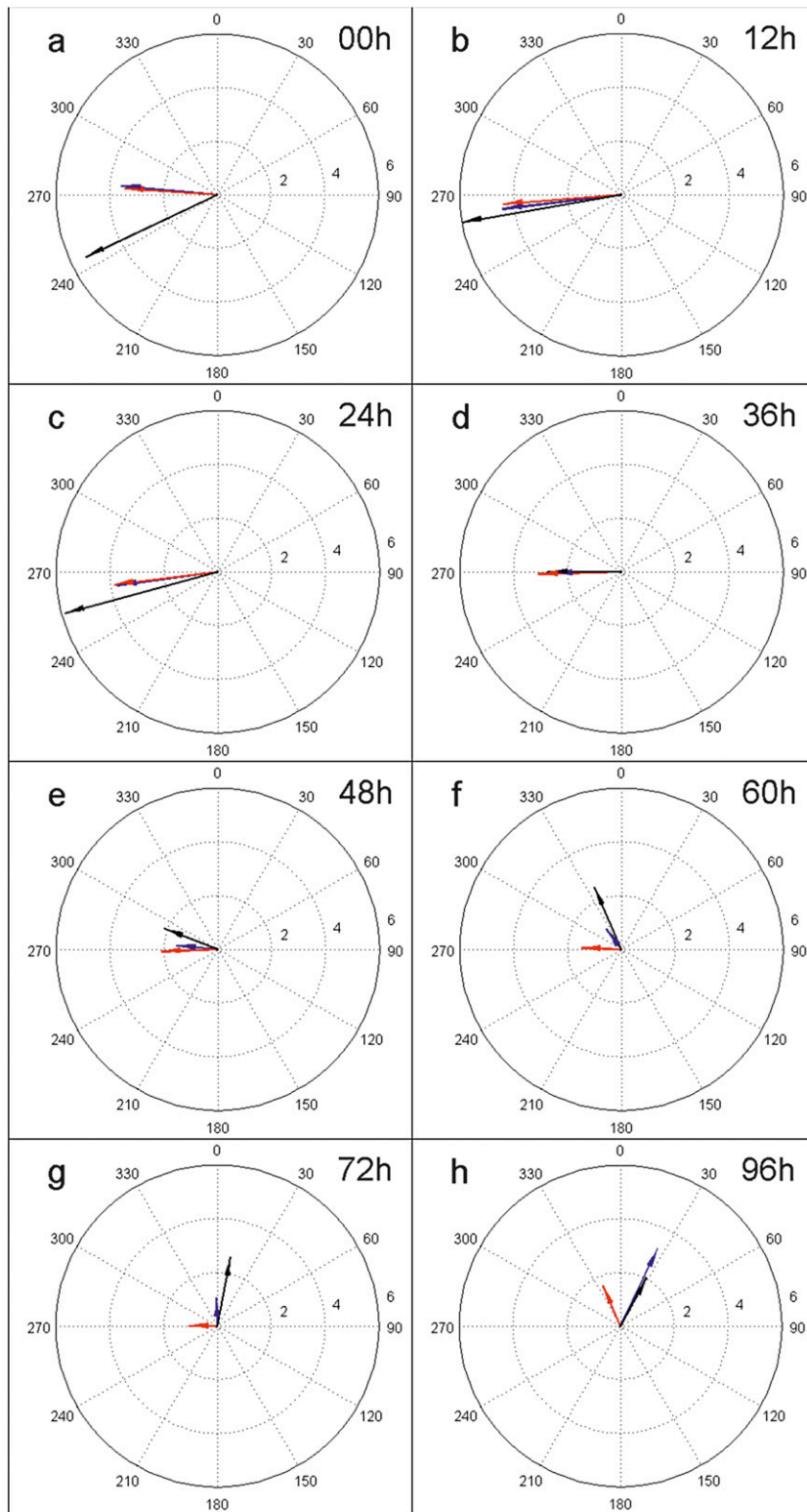


FIG. 11. DLM steering flows over an annulus between 5° and 7° latitude for good members (blue vector) and poor members (red vector) at forecast times of (a) 0, (b) 12, (c) 24, (d) 36, (e) 48, (f) 60, (g) 72, and (h) 96 h with an initial time of 1200 UTC 17 Oct 2010. Rings are spaced every 2 m s⁻¹. Black vector shows true typhoon movement.

are much better than the deterministic forecasts. When facing large uncertainty, forecasters should take advantage of ensemble means and consensus forecasts. Additionally, superensembles, or consensus forecasts based on multiple ensembles, are also an effective way to reduce uncertainty.

TC size is very important in determining its future movement. Unfortunately, numerical models still have difficulty in accurately representing TC structure and size. One way to improve these representations is to use advanced data assimilation algorithms to ingest real-time targeted observations for a better initialization (Jung et al. 2012). Additionally, improvements to the numerical model itself (including the dynamical core and all parameterization schemes) will be needed to ensure that the gains made by data assimilation are not lost during forward integration.

Forecasters must recognize the advantages and disadvantages of global and regional models, including their associated ensemble systems. Based on all newly available sources of data, forecasters should try to learn the differences between the latest updated NWP guidance and real-time observations. Once forecasters can reasonably correct the model output based on these differences, they will be able to determine, a priori, whether the best forecast is likely to be provided by the ensemble mean or by one (or more) of the ensemble members. On the other hand, the operational time constraints may limit the number of ensembles that can be thoroughly diagnosed in real time, a problem that will become even more apparent as the size of ensemble systems increases. Thus, it is very important to develop more objective tools that can help forecasters analyze large numbers of ensembles.

Acknowledgments. The research was mostly conducted during the first author's sabbatical visit at The Pennsylvania State University. We acknowledge the providers of the TIGGE dataset (which is archived and maintained at NCAR) that was used for this study. We thank three anonymous reviewers for their thorough and insightful comments on an earlier version of the manuscript. The research is partially sponsored by the U.S. Office of Naval Research (Grant N000140910526), NOAA through the Hurricane Forecast Improvement Program (HFIP), NSF (Grant ATM-0840651), and by the Typhoon Research Project (2009CB421503) of the National Basic Research Program of China.

REFERENCES

- Adem, J., and P. Lezama, 1960: On the motion of a cyclone embedded in a uniform flow. *Tellus*, **12**, 255–258.
- Aksoy, A., S. Lorsolo, T. Vukicevic, K. J. Sellwood, S. D. Aberson, and F. Zhang, 2012: The HWRF Hurricane Ensemble Data Assimilation System (HEDAS) for high-resolution data: The impact of airborne Doppler radar observations in an OSSE. *Mon. Wea. Rev.*, **140**, 1843–1862.
- Ancell, B., and G. J. Hakim, 2007: Comparing adjoint- and ensemble-sensitivity analysis with applications to observation targeting. *Mon. Wea. Rev.*, **135**, 4117–4134.
- Anthes, R. A., and J. E. Hoke, 1975: The effect of horizontal divergence and the latitudinal variation of the Coriolis parameter on the drift of a model hurricane. *Mon. Wea. Rev.*, **103**, 757–763.
- Bougeault, P., and Coauthors, 2010: The THORPEX Interactive Grand Global Ensemble. *Bull. Amer. Meteor. Soc.*, **91**, 1059–1072.
- Brennan, M. J., and S. J. Majumdar, 2011: An examination of model track forecast errors for Hurricane Ike (2008) in the Gulf of Mexico. *Wea. Forecasting*, **26**, 848–867.
- Buizza, R., J.-R. Bidlot, N. Wedi, M. Fuentes, M. Hamrud, G. Holt, and F. Vitart, 2007: The new ECMWF VAREPS (Variable Resolution Ensemble Prediction System). *Quart. J. Roy. Meteor. Soc.*, **133**, 681–695.
- Cangialosi, J. P., and J. L. Franklin, 2011: 2010 National Hurricane Center forecast verification report. NOAA, 77 pp. [Available online at http://www.nhc.noaa.gov/verification/pdfs/verification_2010.pdf.]
- Chan, J. C.-L., and W. M. Gray, 1982: Tropical cyclone movement and surrounding flow relationships. *Mon. Wea. Rev.*, **110**, 1354–1374.
- , and R. T. Williams, 1987: Analytical and numerical studies of the beta-effect in tropical cyclone motion. Part I: Zero mean flow. *J. Atmos. Sci.*, **44**, 1257–1265.
- Chan, S. T., 2010: Tropical Cyclone Operational Warning Strategies (IWTC-7). WMO/CAS/WWW, 27 pp. [Available online at http://www.wmo.int/pages/prog/arep/wwrp/tmr/otherfileformats/documents/4_3.pdf.]
- Chang, E. K. M., M. Zheng, and K. Raeder, 2013: Medium-range ensemble sensitivity analysis of two extreme Pacific extratropical cyclones. *Mon. Wea. Rev.*, **141**, 211–231.
- Colbert, A. J., and B. J. Soden, 2012: Climatological variations in North Atlantic tropical cyclone tracks. *J. Climate*, **25**, 657–673.
- Dong, K., and C. J. Neumann, 1986: The relationship between tropical cyclone motion and environmental geostrophic flows. *Mon. Wea. Rev.*, **114**, 115–122.
- Elsberry, R. L., 1987: Tropical cyclone motion. *A Global View of Tropical Cyclones*, R. L. Elsberry, Ed., Office of Naval Research, 91–131.
- Fang, J., and F. Zhang, 2012: Effect of beta shear on simulated tropical cyclones. *Mon. Wea. Rev.*, **140**, 3327–3346.
- Fiorino, M., and R. L. Elsberry, 1989: Some aspects of vortex structure related to tropical cyclone motion. *J. Atmos. Sci.*, **46**, 975–990.
- Goerss, J. S., 2000: Tropical cyclone track forecasts using an ensemble of dynamic models. *Mon. Wea. Rev.*, **128**, 1187–1193.
- Hamill, T. M., J. S. Whitaker, D. T. Kleist, M. Fiorino, and S. G. Benjamin, 2011: Predictions of 2010's tropical cyclones using the GFS and ensemble-based data assimilation methods. *Mon. Wea. Rev.*, **139**, 3243–3247.
- Hawblitzel, D., F. Zhang, Z. Meng, and C. A. Davis, 2007: Probabilistic evaluation of the dynamics and predictability of mesoscale convective vortex event of 10–13 June 2003. *Mon. Wea. Rev.*, **135**, 1544–1563.

- Jung, B.-J., H.-M. Kim, F. Zhang, and C.-C. Wu, 2012: Effect of targeted dropsonde observations and best track data on the track forecasts of Typhoon Sinlaku (2008) using an ensemble Kalman filter. *Tellus*, **64A**, 14984.
- Melhauser, C., and F. Zhang, 2012: Practical and intrinsic predictability of severe and convective weather at the mesoscales. *J. Atmos. Sci.*, **69**, 3350–3371.
- Munsell, E. B., F. Zhang, and D. P. Stern, 2013: Predictability and dynamics of a nonintensifying tropical storm: Erika (2009). *J. Atmos. Sci.*, **70**, 2505–2524.
- Qian, C., and Coauthors, 2006: *Grade of Tropical Cyclones*. GB/T 19201-2006, China Standards Press, 10 pp.
- , Y. Duan, S. Ma, and Y. Xu, 2012: The current status and future development of China operational typhoon forecasting and its key technologies. *Adv. Meteor. Sci. Technol.*, **2** (5), 36–43.
- Sippel, J. A., and F. Zhang, 2008: Probabilistic evaluation of the dynamics and predictability of tropical cyclogenesis. *J. Atmos. Sci.*, **65**, 3440–3459.
- , and —, 2010: Factors affecting the predictability of Hurricane Humberto (2007). *J. Atmos. Sci.*, **67**, 1759–1778.
- Velden, C. S., and L. M. Leslie, 1991: The basic relationships between tropical cyclone intensity and the depth of the environmental steering layer in the Australian region. *Wea. Forecasting*, **6**, 244–253.
- Weng, Y., and F. Zhang, 2012: Assimilating airborne Doppler radar observations with an ensemble Kalman filter for convection-permitting hurricane initialization and prediction: Katrina (2005). *Mon. Wea. Rev.*, **140**, 841–859.
- Zhang, F., 2005: Dynamics and structure of mesoscale error covariance of a winter cyclone estimated through short-range ensemble forecasts. *Mon. Wea. Rev.*, **133**, 2876–2893.
- , Y. Weng, J. A. Sippel, Z. Meng, and C. H. Bishop, 2009: Cloud-resolving hurricane initialization and prediction through assimilation of Doppler radar observations with an ensemble Kalman filter. *Mon. Wea. Rev.*, **137**, 2105–2125.
- , —, Y.-H. Kuo, J. S. Whitaker, and B. Xie, 2010: Predicting Typhoon Morakot's catastrophic rainfall with a convection-permitting mesoscale ensemble system. *Wea. Forecasting*, **25**, 1816–1825.
- , —, J. F. Gamache, and F. D. Marks, 2011: Performance of convection-permitting hurricane initialization and prediction during 2008–2010 with ensemble data assimilation of inner-core airborne Doppler radar observations. *Geophys. Res. Lett.*, **38**, L15810, doi:10.1029/2011GL048469.